A&A 419, 385–403 (2004)
DOI: 10.1051/0004-6361:20035779

Astronomy & Astrophysics

Evolutionary design of photometric systems and its application to Gaia

C. A. L. Bailer-Jones[⋆,⋆⋆]

Carnegie Mellon University, Department of Physics, 5000 Forbes Ave., Pittsburgh, PA 15213, USA
Max-Planck-Institut für Astronomie, Königstuhl 17, 69117 Heidelberg, Germany

Received 1 December 2003 / Accepted 19 February 2004

Abstract. How do I find the optimal photometric system for a survey? Designing a photometric system to best fulfil a set of scientific goals is a complex task, demanding a compromise between often conflicting scientific requirements, and being subject to various instrumental constraints. A specific example is the determination of stellar astrophysical parameters (APs) – effective temperature, surface gravity, metallicity etc. – across a wide range of stellar types. I present a novel approach to this problem which makes minimal assumptions about the required filter system. By considering a filter system as a set of free parameters (central wavelengths, profile widths etc.), it may be designed by optimizing some figure-of-merit (FoM) with respect to these parameters. In the example considered, the FoM is a measure of how well the filter system can "separate" stars with different APs. This separation is vectorial in nature, in the sense that the local directions of AP variance are preferably mutually orthogonal to avoid AP degeneracy. The optimization is carried out with an evolutionary algorithm, a population-based approach which uses principles of evolutionary biology to efficiently search the parameter space. This model, HFD (Heuristic Filter Design), is applied to the design of photometric systems for the Gaia space astrometry mission. The optimized systems show a number of interesting features, not least the persistence of broad, overlapping filters. These HFD systems perform as least as well as other proposed systems for Gaia – as measured by this FoM – although inadequacies in all of these systems at removing degeneracies remain. Ideas for improving the model are discussed. The principles underlying HFD are quite generic and may be applied to filter design for numerous other projects, such as the search for specific types of objects or photometric redshift determination.

Key words. instrumentation: photometers – methods: numerical – stars: fundamental parameters – surveys – space vehicles: instruments – stars: general

1. Introduction

Surveys of stellar populations are directed at improving our understanding of their formation and evolution. One of the most important ingredients of such surveys is stellar photometry and/or spectroscopy as a means to determine fundamental stellar parameters. These are, in the first instance, atmospheric parameters – effective temperature, surface gravity and chemical abundances – from which we may derive stellar masses, radii and ages.

A fundamental question facing the designers of such surveys is what spectra and/or photometric systems are optimal for this purpose. Given the constraints of telescope size and survey duration, the designer must generally trade off spectral resolution with signal-to-noise ratio (*SNR*), limiting magnitude, number of sources and sky coverage. Some aspects of the design may be obvious from the scientific goals, but the optimal settings of many others will remain uncertain.

Deep surveys of large numbers of objects will often be forced to employ photometry rather than spectroscopy due to confusion and *SNR* considerations. Given well defined scientific goals, the designer must decide how many filters to use, with what kind of profiles, where to locate them in the spectrum and how much integration time to assign to each. This is usually achieved via a manual inspection of typical target spectra. But if the survey is intended to establish multiple astrophysical parameters (APs) across a large and varied population of objects, then this method of filter design is unlikely to be very efficient or even successful. Manually placing numerous filters and adjusting their profiles to simultaneously satisfy many different – and often conflicting – requirements is likely to be extremely difficult, especially given the vast number of permutations of filter parameters possible. Even if a reasonable filter system could be constructed in this way, we would not know whether a better filter system exists subject to the same constraints. Is there not a more systematic approach to constructing filter systems?

⋆ Emmy Noether Fellow of the Deutsche Forschungsgemeinschaft.
⋆⋆ e-mail: calj@mpia-hd.mpg.de

The approach developed in this article is to use a representative grid of (synthetic) spectra with known APs to construct a filter system in a heuristic fashion. The grid represents the scientific goals of the survey. Let us assume that for a given filter system we can calculate a figure-of-merit which is a measure of how accurately the filter system can determine the APs of the grid spectra. If we consider the filter system as a set of free parameters (central wavelengths, widths, profile shapes etc.), then we may construct a filter system by optimizing the figure-of-merit with respect to these filter parameters. This approach has the advantage that it can exploit the extensive literature on optimization techniques. The specific technique used here is a type of evolutionary algorithm, a population-based technique designed to perform a stochastic yet directed search of the parameter space, adopting features of biological evolution (Sect. 2).

The underlying principle of my approach is to make few prior assumptions about the required filter system and to let the optimization proceed freely within the constraints laid down by the scientific goals and other instrumental considerations.

The model itself, HFD (Heuristic Filter Design), will be described in detail in Sect. 3, but it is worth highlighting now that a crucial aspect is to establish a suitable figure-of-merit. The most obvious would be some average (over the grid) of the precision with which APs are determined. This could be achieved by any one of several regression methods – e.g. nearest neighbours or neural networks – used to approximate the mapping between the data space and the AP space, although doing this well for the multiparameter stellar problem is far from trivial (Bailer-Jones 2002, 2003). Furthermore, because HFD works through many (ca. 10^5) candidate filter systems, fitting a high-dimensional regression model in each case would be unbearably time consuming.

It turns out that an explicit determination of the performance of the filter system in these terms is not actually necessary. A suitable figure-of-merit can be constructed when we consider what a filter system does. Its primary function is to define metrics (e.g. colours) which cluster together similar objects and which separate out dissimilar objects. A simple example is star-quasar separation. If the filter system is designed to determine a continuous AP it should separate objects in proportion to their differences in this AP. In doing this it defines a local vector in the data space along which the AP varies monotonically. (Only once such a separation has been achieved can this vector be calibrated in terms of the AP.) When determining multiple parameters (e.g. $T_{\rm eff}$ and extinction), it is furthermore essential that the local vectors for each parameter are near orthogonal, otherwise a local AP degeneracy exists. Thus "separation" of sources in HFD must be understood in this more general, vectorial sense. Section 3.2 describes how a figure-of-merit is constructed to respect these requirements.

HFD is used in Sect. 4 to design filter systems for the Gaia Galactic Survey Mission and their performance is compared to other proposed systems. Gaia is a high precision astrometric and photometric mission of the European Space Agency to be launched in 2010. Operating on the principles of Hipparcos, but exceeding its capabilities by orders of magnitude, Gaia will determine positions, proper motions and parallaxes for the 10^9 stars in the sky brighter than $V = 20$ (ESA 2000; Perryman et al. 2001). Its primary objective is to study the structure, formation and evolution of our Galaxy. To achieve this, the kinematical information must be complemented with multi-band photometry to determine physical stellar parameters. HFD is used to design appropriate UV/optical/NIR (i.e. CCD) photometric systems for this survey. Section 5 then gives a critical discussion of the HFD approach, its features and limitations and discusses how the approach could be extended and approved. Section 6 summarises the main results and conclusions of this work.

2. Evolutionary algorithms

Many optimization problems can be viewed as the task of finding the values of the parameters of a data model which maximize (or at least achieve a sufficiently large value of) some objective function. Deterministic gradient-based methods are often used, but a major drawback is that they may only sample the parameter space local to the starting point and thus may only find a (suboptimal) local maximum. To overcome this, stochastic optimization methods can be employed in which random (but not arbitrary) steps are taken.

One such method draws upon ideas of natural selection found in biological evolution. In these methods – collectively known as *evolutionary algorithms* – a population of individuals (candidate solutions) is evolved over many generations (iterations) making use of specific *genetic operators* to modify the genes (parameters) of the individuals. The goal is to locate the maximum of some *fitness* function (figure-of-merit). As a population-based method, it takes advantage of evolutionary behaviour (breeding, natural selection, maintenance of diversity etc.) to perform more efficient searches than single solution methods (e.g. simulated annealing).

A fairly generic evolutionary algorithm (EA) proceeds as follows. We start with an initial population of μ individuals, perhaps generated at random. From these, we generate an intermediate population of λ individuals ($\lambda \geq \mu$) either via *recombination* – the breeding of individuals to produce offspring with different combinations of their parameters – and/or via *mutation* – the application of small random changes to individuals' parameters. The μ fitter individuals from this intermediate population are then selected. This *selection* could be carried out deterministically – take the best μ – or probabilistically, e.g. by selecting (with replacement) individuals from the parent population with a probability proportional to their fitness. The procedure is then iterated. At any generation we have μ different solutions to our optimization problem. Just as is believed to take place in biological evolution, the evolution of the system is not directed step-by-step, but rather the population as a whole improves itself through the constant reproduction of new individuals and the natural selection of the fitter ones. A brief discussion of the different types of EAs plus references to the literature is given in Appendix B. The specific genetic operators used in HFD are described in the next section.

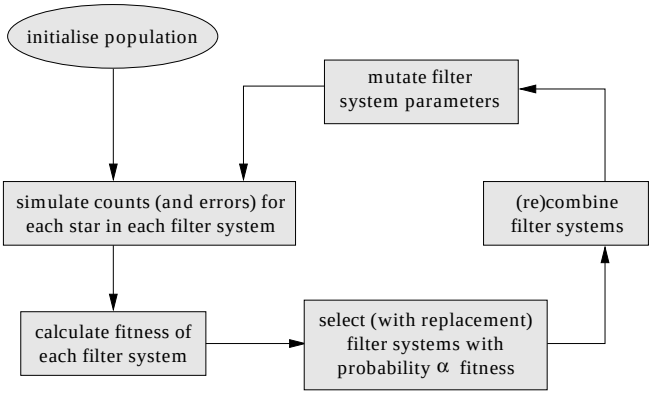

Fig. 1. Flow chart of the core aspects of the HFD optimization algorithm. A single loop represents a single iteration, i.e. the production of one new generation of filter systems.

3. The HFD model

The goal of HFD is to design a survey photometric system according to how well it can separate stars with different astrophysical parameters (APs) and avoid degeneracy between the APs. The filter system is developed for a specific survey, the scientific goals of which are represented by a grid of stars with specified APs, magnitudes and spectral energy distributions (SEDs). From these and the instrument model, HFD calculates the fitness of each filter system and uses this to evolve the population. This iterative optimization procedure is summarized in Fig. 1. The critical aspects of HFD are now described: the filter system representation (Sect. 3.1); the fitness measure (Sect. 3.2); the genetic operators (Sect. 3.3).

3.1. Filter system representation and instrument assumptions

To be amenable to optimization, the filter system must be parametrized, or "represented". This representation is influenced by constraints, or fixed parameters, within which the optimization proceeds. These relate primarily to the instrument.

I first assume that the aperture size (primary mirror area) is fixed according to financial, technical and other scientific constraints. Second, I assume that (a) a fixed total amount of integration time is available for each source to be observed, and that (b) this is the same for each source. The total integration time per source depends upon the survey duration, the field-of-view of the instrument, the area to be observed, and the scanning law (how the field-of-view maps the sky with time). A uniform scanning law ensures conditions (a) and (b). Although this is not actually true for Gaia, it is a reasonable simplifying approximation. Third, I assume that the total integration time per source must be divided among all filters. This is the case for Gaia (and, for example, SDSS) in which the focal place is covered with a two dimensional array of CCD detectors arranged in one dimensional strips, with different filters attached directly to different strips. As the instrument scans the sky the stars cross the focal plane perpendicular to these strips and the CCDs are clocked at the same rate. The integration time in each filter is therefore set by the width of its respective CCD strip. Finally, the wavelength response of the instrument (throughput) and the detectors (quantum efficiency) are specified and held constant during the optimization.

Each filter in a filter system is parametrized by the following three parameters: the central wavelength, c, the half-width at half maximum (*HWHM*), b, and the fractional integration time, t, i.e. the fraction of the total integration time (per source) allocated to this filter. The profile of every filter is given by the generalized Gaussian

$$\Psi(\lambda) = \Psi_0 \exp\left[-(\ln\ 2)\left|\frac{\lambda - c}{b}\right|^{\gamma}\right]. \quad (1)$$

This is Gaussian for $\gamma = 2$, and rectangular for $\gamma = \infty$. Values between these give Gaussian-like profiles but with flatter tops and steeper sides. $\gamma = 8$ is adopted throughout. A fixed peak throughput of $\Psi_0 = 0.9$ is used.

For a system of I filters, there is a total of $3I$ filter system parameters: these are the free parameters with respect to which the optimization is performed. More complex filter parametrizations are of course possible. For example, additional parameters could allow the shape, steepness or asymmetry of each profile to be optimized. The philosophy adopted here is to use a simple parametrization consistent with a reasonably realistic profile.

The fractional integration time is taken as a real number, $0.0 \le t_i \le 1.0$, and must of course be normalized, $\sum_i t_i = 1.0$. Realistically, CCDs would not be used with arbitrary widths and hence arbitrary values of t. This could be accommodated by rounding final values of t or by using a discrete representation (see Sect. 4.3.1).

Given the filter profiles and the fixed instrument parameters, the number of photons detected in each filter from each source are simulated. The fitness function also requires the expected photometric noise. HFD assumes three noise sources: (1) Poisson noise from the source; (2) Poisson noise from the background (two contributions: one over the source and the other arising from the need to do background subtraction); (3) CCD readout noise.

In the present implementation, the number of filters, I, is fixed. HFD could be generalized to optimize this at the expense of algorithm complexity. But as we generally consider small values of I (ca. 5–20), I simply run separate optimizations for different values of I and compare the fitnesses. Furthermore, during the optimization HFD is able to "turn off" filters by assigning $t = 0$ to a filter, thus reducing the number of effective filters.

3.2. Fitness measure

The fitness measure is a vital part of the optimization procedure and was qualitatively described in Sect. 1. Not only must it characterize how well the filter system performs, but it must do this in such a way that it is appropriately sensitive to all of the APs. In fact, the most significant challenge in constructing a fitness function for this problem was taking into account *multiple* astrophysical parameters, in particular parameters which have very different magnitude effects on the data and which

may be degenerate. This is certainly the case for the four APs considered in the Gaia application, $T_{\rm eff}$, $\log g$, [Fe/H] and $A_{\rm V}$.

The fitness function can be considered in three parts, the *SNR-distance*, the *AP-gradient* and the *orthovariance*, which I now describe.

With I filters, the R sources in the grid define R points in an I-dimensional space, the *data space*. Let the expected (i.e. noise free) number of photons detected from the rth source in the ith filter of the kth filter system be $p_{k,i,r}$, and let the standard deviation in this (from the noise model) be $\sigma_{k,i,r}$. These values are normalized to sources of equal brightness (see below). The *SNR-distance* between source r and a neighbouring source n is defined as

$$d_{k,r,n} = \sqrt{\left[\sum_{i=1}^{i=I} \frac{(p_{k,i,r} - p_{k,i,n})^2}{\sigma_{k,i,r}^2 + \sigma_{k,i,n}^2}\right]}. \quad (2)$$

Without the denominator, this expression would simply be the Euclidean distance between sources r and n. The denominator modifies this distance to be in units of the combined noise of the two sources (standard deviations added in quadrature in the case of small, uncorrelated noise). If we were designing a filter system to discretely classify two or more classes of objects, a suitable fitness measure would be the average of $d_{k,r,n}$ over all non-similar neighbours, n, (i.e. all sources in the other classes), and summed over all sources, r.

The *SNR*-distance is defined in terms of normalized photon counts to ensure that it is zero for identical SEDs differing only in apparent magnitude. Source SEDs are normalized such that they all have the same counts in the G band, the "white light" band used for the astrometric instrument on Gaia (see Sect. 4.2).

We now need to introduce sensitivity to the APs. For a given *SNR*-distance between two stars, r and n, the larger their AP difference, the less fit is the filter system. This is quantified with the *AP-gradient*, which for the jth AP is defined as

$$h_{k,r,n,j} = \frac{d_{k,r,n}}{|\Delta\phi_{j,r,n}|} \quad (3)$$

where $\Delta\phi_{j,r,n} = \phi_{j,n} - \phi_{j,r}$ is difference in the jth AP between sources r and n. To remove the absolute units of the APs, each AP is scaled to lie in the range 0–1.

We might think that we could generalize Eq. (3) to account for multiple APs by simply summing over j, suitably weighting each term to account for the fact that small changes in some parameters (e.g. $T_{\rm eff}$ and extinction) produce larger changes in the SED than others (e.g. [Fe/H] and $\log g$). However, this does not address the degeneracy between the APs, i.e. it ignores the fact that changes in $d_{k,r,n}$ introduced by varying one AP can be replicated by varying another AP. Such a measure would therefore be blind to the *individual* effects of each AP on the SED. As all four APs considered here have broad band (pseudo-)continuum effects on the SED (see Fig. 8) this is a significant issue[1].

[1] In principle, narrow band filters measuring individual lines sensitive to specific APs could overcome some degeneracies, but this is unlikely to be acceptable for a large, deep survey. Moreover, a fitness measure explicitly sensitive to AP-degeneracy can quantify this, as demonstrated in Sect. 4.4.

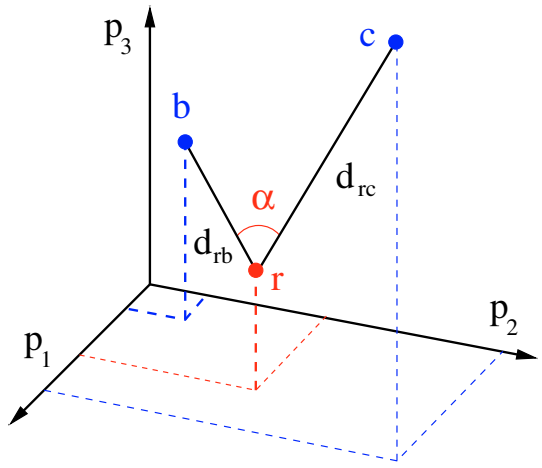

Fig. 2. Principle of orthovariance illustrated for a three dimensional data space p_1, p_2, p_3. For a given source, r, the neighbours b and c, which differ from r only in astrophysical parameters (APs) j and j' respectively, are found. These are *isovars* ("isolated variance") of r for APs j and j' respectively. The vectors ***rb*** and ***rc*** are local linear approximations to the *principal directions*, those directions in which the APs vary at r. The angle between the vectors is α. The closer to orthogonal these vectors are the better the vector separation (and hence the lower the degeneracy) between these two APs at r.

A filter system free of this degeneracy is one in which the direction in the data space in which one AP varies (locally) is orthogonal to the directions in which all other APs vary. I call these local vectors the *principal directions*, demonstrated for a three dimensional data space in Fig. 2. These directions are approximated by the vectors ***rb*** and ***rc*** connecting source r to neighbouring sources b and c respectively. Source b differs from r only in AP j; source c differs from r only in AP j'. (A source which differs from r in only one AP is called an *isovar* – for "isolated variance" – of r.) Let the angle between these two vectors be $\alpha_{r,j,j'}$. The nearer this angle is to 90°, the lower the degeneracy between APs j and j' at r, and thus the better the filter system. The nearer $\alpha_{r,j,j'}$ is to 0° or 180°, the poorer the filter system is at distinguishing between the effects of the APs, no matter how large the AP-gradients. Hence a suitable fitness measure could be proportional to $\sin\alpha_{r,j,j'}$.

This concept, which I call *orthovariance*, can be extended to any number of APs. For J APs we have $J(J-1)/2$ unique pairings of principal directions at a point and this number of $\sin\alpha$ (orthovariance) terms.

We now have two distinct figures-of-merit for the performance of a filter system: the AP-gradients and the orthovariance terms. For the single objective optimization approach of HFD, these need to be combined into a single fitness function. This is done as follows. The fitness of filter system k on source r is defined as

$$f_{k,r} = \sum_{j,j'\neq j} x_{k,r,j,j'} \quad (4)$$

which consists of $J(J-1)/2$ terms given by

$$x_{k,r,j,j'} = h_{k,r,n_j}\, h_{k,r,n_{j'}} \sin\alpha_{k,r,j,j'} \quad (5)$$

$$= \frac{d_{k,r,n_j}\, d_{k,r,n_{j'}} \sin\alpha_{k,r,j,j'}}{|\Delta\phi_{j,r,n_j}|\,|\Delta\phi_{j',r,n_{j'}}|}. \quad (6)$$

The term d_{k,r,n_j} is the *SNR*-distance, where n_j means the nearest neighbour to r which differs only in AP j (i.e. source $b \equiv n_j$ in Fig. 2), and similarly for $d_{k,r,n_{j'}}$. "Nearest" is in terms of the *SNR*-distance. The form of Eq. (6) is motivated by the observation that the numerator is simply the magnitude of the cross product between the two vectors $\boldsymbol{rb}$ and $\boldsymbol{rc}$, with the denominator converting these vectors to AP-gradients. The sum in Eq. (4) is over all pairs of APs. As the AP gradients are calculated using neighbours which differ in only one AP, they are simply the first order difference approximations of the derivatives of the *SNR*-distance with respect to each AP at point r in the grid. The nominal fitness for filter system k is then the sum over all sources

$$F_k = \sum_r f_{k,r} \tag{7}$$

$$= \sum_{j,j'\neq j} \sum_r x_{k,r,j,j'}. \tag{8}$$

As the sources are synthetic spectra, they can be set up on a sufficiently regular grid to ensure that most sources have isovars. Some sources may not have isovars for some APs, in which case those terms in Eqs. (4) and (8) cannot be calculated and are omitted. This is the case for some sources/APs in the grid used later (Table 4.1).

Equation (8) could be used directly as the fitness function if it were not for the fact that it suffers from two problems: AP dominance and a low sensitivity to orthogonality.

To address the former we must appreciate that some APs have a more pronounced effect on the data than others, i.e. a given $\Delta\phi$ for some APs (A_V and $T_{\rm eff}$) will produce a much larger change in the *SNR*-distance than other APs ($\log g$ and [Fe/H]). (Recall that ϕ is scaled to the range 0–1 for each AP.) Thus $f_{k,r}$ and hence F_k will be dominated by a subset of APs and will show little sensitivity to others, with the result that filter systems are optimized essentially in ignorance of these "weaker" APs. This may be overcome by multiplying each AP-gradient term by a factor, w_j, to bring the AP-gradients for each AP to a common level. These factors are determined by examining the distribution of the AP-gradients for typical filter systems produced by HFD. Even with these, the fitness may be dominated by large values of the AP-gradient for a few sources (so-called "overseparation"). To mitigate this, the AP-gradients may be raised to a power $1/n$ for $n > 1$; $n = 2$ is used.

The second problem which arises is as follows. While the cross product interpretation of Eq. (6) is appealing, it overlooks the fact that, for example, values of $\sin\alpha$ up to 0.95 occur for angles only up to 72°, yet, intuitively, vectors separated by 90° ($\sin\alpha = 1.0$) should be considerably more than 1.0/0.95 times fitter. Consequently, I down weight values of $\sin\alpha$ less than 0.95. This is done with a two-component linear transfer function, consisting of a line joining $(0,0)$ to (x_0, y_0) and another joining (x_0, y_0) to $(1,1)$, i.e.

$$T(\sin\alpha) = \left(\frac{y_0}{x_0}\right)\sin\alpha \qquad \text{if} \quad \sin\alpha < x_0$$

$$= \left(\frac{1-y_0}{1-x_0}\right)(\sin\alpha - x_0) + y_0 \quad \text{otherwise} \tag{9}$$

with the transition point $(x_0, y_0) = (0.95, 0.1)$. Generally speaking, the value of the transmission point, x_0, should depend on both the dimensionality of the data space, I, and the number of principal directions, J, because the occurrence and extent of degeneracies depends on these. For simplicity this fixed value is used throughout this article.

Incorporating these two modifications and converting the sums to be averages (to make the fitness invariant with respect to the number of sources)[2], the final fitness measure is

$$F_k^* = \frac{2}{J(J-1)} \sum_{j,j'\neq j} \frac{1}{R} \sum_r x^*_{k,r,j,j'} \tag{10}$$

where

$$x^*_{k,r,j,j'} = w_j (h_{k,r,n_j})^{1/2}\, w_{j'} (h_{k,r,n_{j'}})^{1/2}\, T(\sin\alpha_{k,r,j,j'})$$

where the scale factors are normalized such that $\sum w_j = J$. The fitness has units of an AP-gradient per source per AP pair multiplied by a dimensionless orthovariance factor.

Some aspects of this modified fitness function may seem ad hoc. However, it was found through detailed experimentation that such modifications were necessary to increase the sensitivity of the fitness function. Further discussion of this point is given in Appendix A.

Some properties of the fitness should be noted. In the limit where Poisson noise from the source is dominant (the "bright star limit"), the *SNR*-distance, d, is scale invariant with respect to the number of filters, I, in the sense that for a flat spectrum and CCD/instrument response the fitness is independent of the number of (equal *HWHM*) filters. This is relevant because it means that the fitnesses of filter systems with different numbers of filters can be directly compared. In the bright star limit, the *SNR*-distance is linearly proportional to the *SNR*. As long as this limit holds, the HFD optimization is independent of source magnitude (because the genetic selection operator is invariant with respect to multiplicative scalings of the fitness). In the faint star limit – where source-independent noise terms dominate – $d \propto 1/\sqrt{I}$. In other words, at faint magnitudes there is a penalty to be paid for retaining a large number of filters, something which is seen in the applications in Sect. 4.

3.3. Genetic operators

The evolutionary aspects of EAs which distinguish them from random searches are embodied in the genetic operators. The principal operators are *selection*, *recombination* and *mutation* (see Fig. 1). Between them, these operators provide for an exploration of the parameter space (mutation and recombination) and an exploitation of the fitter solutions (selection).

3.3.1. Selection

Selection is performed probabilistically via the commonly-used "roulette wheel" method: Each individual is selected from

[2] As some sources do not have isovars they are dropped from the summation over r and the normalization factor, R, is correspondingly reduced.

the parent population with a probability proportional to its fitness (Eq. (10)). As selection is done with replacement, the expectation is that individuals are selected with a frequency proportional to their fitnesses. Note that we do not simply retain the fittest individuals at each generation. While this would guarantee a monotonic increase in the maximum fitness, it would rapidly erase diversity in the population resulting in premature convergence to a poor local maximum. Even so, with a finite population there is a chance that the best individuals are not selected and that improvements in fitness from earlier generations are lost. To guard against this, *elitism* is used: the E fittest individuals ($E < K$, where K is the population size) are copied to the next generation without modification. The remaining $K - E$ individuals for the next generation are selected probabilistically from the full parent population (including the E elite), and combined/mutated in the normal way. We shall see in Sect. 4.3.2 that elitism produces significant performance gains.

3.3.2. Recombination

After an individual has been selected, it is (re)combined with a probability P_r with a second selected individual. This is done by randomly selecting one filter from each system and swapping them. A value of $P_\mathrm{r} = 1/3$ is used on the basis that the expected fraction of offspring produced by recombination is then 0.5. It turns out (Sect. 4.3.2) that HFD is very insensitive to P_r and that this operator is actually unnecessary.

3.3.3. Mutation

After selection (and possibly recombination) each parameter (c, b and t) of each filter is mutated with a probability P_m. A mutation is a random Gaussian perturbation. For the central wavelength, the mutation is additive: $c \to c + N(0, \sigma_c)$. For the filter width and fractional integration time, the mutation is multiplicative: $b \to b(b > 0,\, N(1, \sigma_b))$ and $t \to t(t > 0,\, N(1, \sigma_t))$. As $\sigma_b < 1.0$, σ_b can be considered as the typical fractional change in b, and likewise for t. Whereas linear changes in the central wavelength seem an appropriate way of sampling that parameter, changes proportional to the current size of the parameter seem more appropriate for the *HWHM* and fractional integration time.

HFD operates within both absolute wavelength limits defined by the CCD/instrument profile and wavelength limits on the *HWHM*, such that mutations which would violate these limits are not accepted (see Sect. 3.4). Limits are also applied to the fractional integration time. A minimum is applied such that if a mutation sets a value of t below t_min then t is set to zero. The filter can be turned on again by any successful positive mutation. Thus while the number of filters in the model is fixed, the number of *effective filters*, i.e. filters with $t > 0$, is variable. This lower limit on t was imposed to prevent very short integration times, which would require unrealistically narrow CCDs. Likewise, mutations which would take t above t_max are rejected. For I filters, I use $t_\mathrm{min} = 1/(4I)$ and $t_\mathrm{max} = 4/I$ but with the latter truncated to a maximum of 0.5. Experimentation has shown that this upper limit on t is probably not necessary, because the fitness function itself penalizes such solutions through the lack of integration time it permits for other filters.

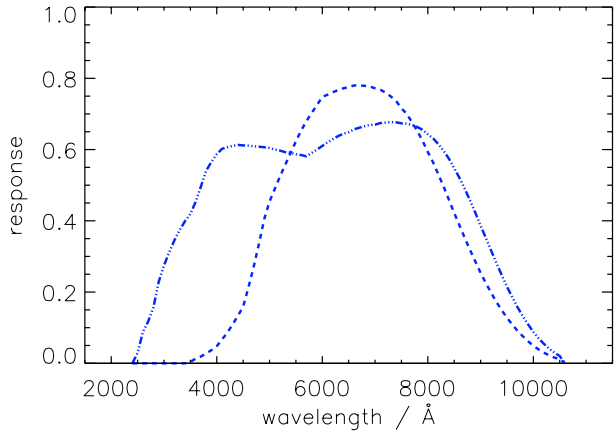

Fig. 3. Responses (CCD quantum efficiency multiplied by instrument throughput) for the BBP instrument (dashed line) and the MBP instrument (dot-dashed line). The instrument responses are six reflections of silver and three of aluminium respectively. The BBP response defines the G band, which, along with the AB system, defines the magnitude system adopted for Gaia. The MBP response is a composite of two different CCD QE curves (joined at 5700 Å where they have equal QE).

For the evolutionary search mechanisms to be superior to a random search we must assume that the fitness is a smooth function of the filter system parameters over some reasonable length scale. The mutation sizes should be comparable to these length scales; if they were much larger then the childs' fitness would not correlate with its parents' fitness and the search would be quasi-random. Quantifying these length scales is not straight forward without knowledge of the shape of the fitness landscape. A typical mutation size should obviously be much smaller than the total range of a parameter and from our astrophysical knowledge we can also say that mutations below some value will have negligible effect. Based on such considerations as well as experimentation, the values of σ_c, σ_b and σ_t were fixed at 500 Å, 0.50 and 0.25 respectively. Experimentation has found that the results of HFD are not very sensitive to these values (see Sect. 4.3.2). Likewise, the evolution is not very sensitive to P_m, which was set to 0.4.

3.4. HFD initialization and execution

The population is initialized by drawing c and b at random from a uniform distribution between the minimum and maximum values of these parameters. The permissible wavelength range is determined by the CCD/instrument response (Fig. 3), and is is set to 2750−11 250 Å for BBP and 1750−11 250 Å for MBP (the two instruments on Gaia; see Sect. 4.2). These are extended compared to the zero response values to permit cut-off filters. The permitted range for the *HWHM* is set at 80−4000 Å. The lower limit is introduced to avoid errors interpolating the SEDs (and very narrow filters are anyway not acceptable on *SNR* grounds). The upper limit is essentially no limit as it encompasses the entire permissible wavelength range. Interestingly, the optimization naturally constrains itself

Table 1. HFD parameter overview. The optimization is done with respect to the $3I$ free parameters (with bounds). Symbols for parameters are given where used in the text. The nominal parameter values used in the simulations described in Sect. 4 are listed. The two sets of instrument parameters labelled "BBP" and "MBP" refer to the two Gaia instruments described in Sect. 4.2.

Free parameters			
central wavelength/Å	c	$\times I$	
full-width at half maximum/Å	b	$\times I$	
fractional integration time	t	$\times I$	
Fixed parameters: fitness measure			
stellar population (number of sources, $R = 415$)		Table 2	
magnitude of stars (in G band)[1]		15	
AP weight A_V		1.5/128	
AP weight [Fe/H]		75.0/128	
AP weight $\log g$		50.0/128	
AP weight $\log T_{\rm eff}$		1.5/128	
Fixed parameters: evolutionary algorithm			
number of filter systems (=population size)	K	200	
size of elite	E	10	
number of generations		200	
number of runs[2]		20	
probability of recombination	$P_{\rm r}$	1/3	
probability of mutation	$P_{\rm m}$	0.4	
std. dev. of mutation for c/Å	σ_c	500	
std. dev. of mutation for b	σ_b	0.5	
std. dev. of mutation for t	σ_t	0.25	
Fixed parameters: instrumental		**BBP**	**MBP**
filter profile		Eq. (1)	Eq. (1)
number of filters	I	5	10
telescope aperture area/m^2		0.7	0.25
total integration time/s		1205	16 500
CCD & instrument response		Fig. 3	Fig. 3
CCD readout noise/e$^-$		251	277
effective background/G mag		22.37	18.29
min.(c-b), max.(c+b) / Å		2750, 11 250	1750, 11 250
min. b, max. b/Å		80, 4000	80, 4000
min. t, max. t	$t_{\rm min}$, $t_{\rm max}$	0.05, 0.5	0.025, 0.4

[1] The G band is defined in Sect. 4.2. The stars do not in general have to have the same magnitude.
[2] The number of independent runs of HFD from different initializations is not a parameter of the model.

to a more limited range of *HWHM* (Sect. 4). The fractional integration times are initialized to be equal (to $1/I$).

The evolution is terminated after a fixed number of generations, typically 200, beyond which the rate of increase of fitness in numerous configurations was found to be very small. This entire optimization process is repeated for a number of *runs* commencing from different initializations to investigate how consistently HFD converges on a common solution (sensitivity to initial conditions).

The parameters involved in HFD are summarized in Table 1, where the values for the "nominal" optimizations in Sect. 4 are also given. What little theory exists to guide us in setting the parameters of the EA is derived from very simple problems which may have little generality. One is therefore forced to perform tests and build up experience of the sensitivity of the model to these parameters. A population size of 200 and an elite of 10 was selected somewhat arbitrarily: the effect of varying these and other parameters will be discussed below.

4. Application of HFD to the design of Gaia filter systems

HFD is applied to design photometric systems for two Gaia instruments. In both cases the goal is to achieve systems which can best determine the four astrophysical parameters, effective temperature ($T_{\rm eff}$), surface gravity ($\log g$), metallicity ([Fe/H]) and interstellar extinction[3] (A_V), for a grid of stars.

[3] Extinction is not an intrinsic stellar property, but as extinction can vary considerably on small spatial scales it should ideally be determined for each star individually.

Table 2. The stellar grid in $T_{\rm eff}$ and $\log g$ (spectral types are given for guidance). Each of these 17 AP combinations is reproduced at the five metallicities and five extinctions shown at the bottom of the table, giving a total of 425 sources (some metallicities are missing from the Basel library, so there are actually only 415 sources).

$\log g$	$T_{\rm eff}$/K (SpT)						
4.5	3500 MV	4750 KV	5750 GV				
4.0				6750 FV	8500 AV	15000 BV	35000 OV
3.5							
3.0				6000 RRLyr	8500 BHB		
2.5			5500 GIII			15000 BIa	
2.0		4500 KIII	5500 FIa				
1.5					8500 AI		
1.0	3500 MIII		5000 GI				
0.5							
0.0	3500 MIa						
	[Fe/H] =		+0.5	0.0	−0.5	−1.5	−2.5
	$A_{\rm V}$ =		0.0	0.2	2.0	5.0	10.0

4.1. The stellar grid

The main purpose of the grid is to sample the dependence of the SED on the APs in order to calculate the fitness, and from this perspective it is not necessary to have a very dense grid (but see Sect. 5). The grid used is shown in Table 2. It has been constructed loosely considering the scientific goals of Gaia. The SEDs are Basel2.2 synthetic spectra (Lejeune et al. 1997) which were artificially reddened using the curves of Fitzpatrick (1999) with $R_{\rm V} = 3.1$.

For a given optimization, all stars are presented at the same magnitude in the G band (see Sect. 4.2). The nominal optimization is carried out at $G = 15$, the target magnitude for Gaia (ESA 2000). Section 4.3.2 demonstrates the effect of varying this magnitude. Note that the SEDs themselves are noise free: the magnitude at which they are presented determines the noise in the *SNR*-distance (Eq. (2)). All magnitudes are on the AB system (Oke & Gunn 1983).

By necessity, this grid is a simplification of the true diversity of scientific targets which Gaia will encounter. Many more sources and additional astrophysical parameters could be included, and done so at characteristic magnitude ranges.

4.2. The Gaia instrument model

Gaia employs two separate telescopes (focal planes; see Sect. 3.1) each equipped with different instruments (see ESA 2000 or Perryman et al. 2001, although the designs have since been slightly modified and may well be modified again). The first instrument is the astrometric instrument comprising a large array of unfiltered CCDs. This pass band – called the *G band* – is defined by the CCD/instrument response. The centroid of the point spread function through this broad band is colour dependent, so to achieve accurate astrometry a chromatic correction is required. This is supplied by a number of (typically) broad band filters on the trailing edge of the focal plane, referred to as the *Broad Band Photometer*, BBP. It turns out that provided there are four or five filters covering the G band, we are free to optimize BBP for other purposes (Lindegren 2001), e.g. stellar parametrization. As focal plane area is limited in this instrument, a second instrument, the *Medium Band Photometer*, MBP, exists, the primary goal of which is stellar parametrization. It works on the same principle as BBP, and although it has a smaller telescope aperture than BBP, it has a much larger area and field of view, so more filters can be allocated. Current designs for MBP have considered 8–11 bands.

The instrument models used here for MBP and BBP reflect the Gaia designs as of mid 2003. The main parameters are summarized in Table 1 (for end-of-mission, i.e. multiple scans). Each instrument has a different wavelength response and uses different CCDs (Fig. 3). MBP additionally has red- or blue-enhanced CCDs depending on the filter central wavelength. For simplicity, a composite of these two is used in HFD by taking the maximum of each QE profile. For the noise model, a background with solar SED and $V = 22.50$ ($G = 22.18$) mag/sqarcsec is assumed (ESA 2000). This is translated to background counts in the source extraction using aperture photometry, yielding the effective background in Table 1. The large background for MBP is a result of optical aberrations (from the short focal length) giving rise to poor spatial resolution necessitating a large extraction aperture. This will also produce source

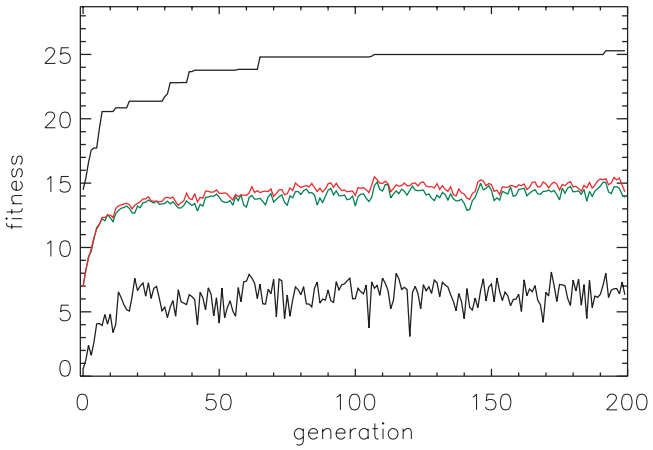

Fig. 4. Evolution of fitness statistics for a typical HFD run applied to the nominal BBP model. The lines from top to bottom denote the maximum, mean, median and minimum fitness in the population.

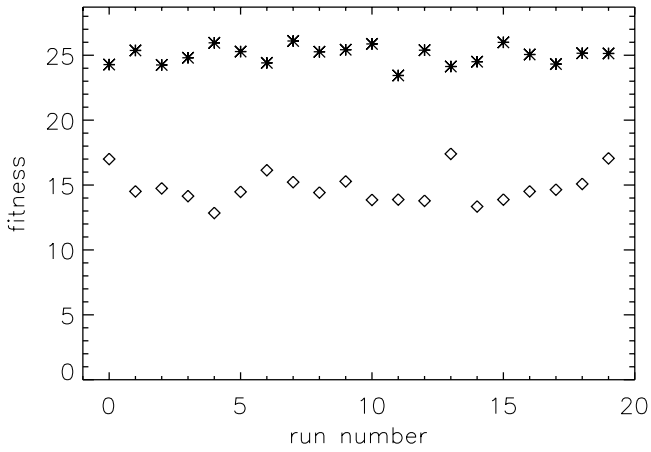

Fig. 5. Maximum fitness in the initial random population (diamonds) and in the final population (stars) for each of 20 independent BBP runs.

confusion at brighter magnitudes than occurs with BBP. Due to these different characteristics, a joint optimization of the MBP and BBP filter systems is probably not desirable.

While the terms BBP and MBP will be retained for these instruments, it should be noted that the HFD optimization sets essentially no limits on the *HWHM* of the filter profiles (Sect. 3.4).

4.3. Results: BBP

The first part of this section examines in detail the optimization of a 5-filter BBP system using the nominal settings in Table 1. The second part examines the effect of varying these parameters.

4.3.1. Nominal model parameter settings

The typical evolution of the fitness during an optimization run is shown in Fig. 4. Starting from the initial random population, we see a rapid increase in all fitness statistics over the first few generations followed by a slower increase over the rest of the evolution. The mean and median, always very close, oscillate around a constant value after 20–40 generations. The minimum value shows similar behaviour, but with larger negative dips indicating the creation of poor solutions. In contrast, the maximum fitness never decreases, as guaranteed by elitism (Sect. 3.3.1). Significantly, the maximum fitness continues to increase after the other measures have levelled off, although by decreasing amounts: while the population as a whole "stagnates", a few ever fitter individuals continue to be created. This is what is important, as the goal of the evolutionary algorithm in this problem is to achieve the highest fitness of a single individual (the *run maximum*), rather than improve the whole population. The increase in maximum fitness after 200 generations looks asymptotic. Extending the evolution to ten times as many generations only improves the run maximum fitness by around 2%.

Figure 5 shows that the run maximum fitness is fairly consistent across runs, the spread across 20 runs being about 10%. It further shows that the improvement in maximum fitness as a result of using the search and selection operators (as opposed to random search) is a factor of about 1.8.

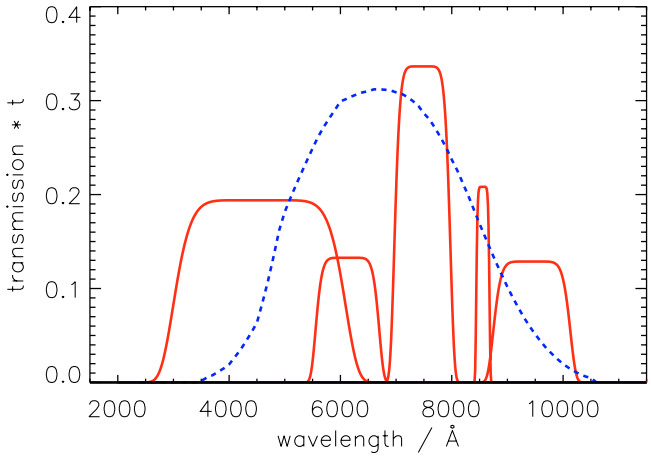

Fig. 6. The HFD-1B filter system, a BBP filter system produced by HFD (run No. 7 – the fittest run – in Fig. 5). The peak filter transmissions have been scaled to the fractional integration time for each filter (the true peak transmission of each filter is fixed at 0.9). Thus the exact points of overlap of the filters are not accurately depicted. The dashed line shows the instrument+CCD response curve for BBP, arbitrarily scaled in the vertical direction. The filter parameters are listed in Table 3.

Figure 6 shows the best filter system produced from these 20 runs. A number of features are immediately apparent. First, the filters cover the entire wavelength range, and four of the five filters are rather broad. Second, the reddest and bluest filters extend essentially to the longest and shortest wavelengths possible with the instrument response, i.e. they are cut-off filters. Third, all five filters have non-zero integration time. These general features are consistently found in the run maxima of the 20 runs, and the best five runs in particular produce very similar filter systems. An indication of the overall consistency is given in Fig. 7, where six filter systems ranging from the fittest to least fit run maxima across the 20 runs are shown. More significant differences occur among the less fit systems, e.g. the lack of a red cut-off filter, or more significant

Table 3. Parameters for the filters in the HFD-1B (BBP) and HFD-1M (MBP) filter systems according to the filter parametrization given in Sect. 3.1. Wavelengths are reported to ±5 Å. In a practical implementation, filters with profiles extending beyond the CCD QE cutoff would be truncated, thus altering c and b.

		c/Å	b/Å	t
HFD-1B	1	4545	1505	0.194
	2	6125	555	0.133
	3	7470	490	0.336
	4	8560	115	0.208
	5	9440	675	0.129
HFD-1M	1	2870	660	0.056
	2	3810	175	0.079
	3	4825	870	0.134
	4	5345	1130	0.298
	5	8520	205	0.125
	6	9355	1120	0.187
	7	9375	495	0.120

overlap of filters. In two cases there are only four effective filters (i.e. the fifth has $t = 0$) and in another case two filters are almost identical. While HFD appears to converge toward a stable filter system, no convergence criterion is used to terminate the evolution. The differences between the final filter systems (and fitnesses) of each run could, therefore, reflect incomplete convergence as much as convergence on different local maxima of the filter parameter space.

A consistent aspect of HFD – seen for many variations of the grid, instrument and EA parameters – is that it produces systems with broad filters. At first this seems counterintuitive, as we may expect the best distinction between stellar parameters to be achieved by placing narrow filters on specific (narrow) features. Inspection of the fitness function, Eq. (10) and in particular the *SNR*-distance component (Eq. (2)), gives some explanation. For constant values of $\sin\alpha$, the fitness can be increased by making the filters wider. This increases the *SNR* so is obviously desirable. If this widening increases the degeneracy between APs then it is penalized through a reduction in the value of $\sin\alpha$ and thus a decrease in the fitness. We can think of HFD as attempting to simultaneously achieve the largest values of the *SNR*-distance (or rather, the AP-gradients) between sources consistent with also maximizing their vector separation (Fig. 2). That this is functioning at some level is indicated by the fact that although the filter half widths can extend up to (and are initialized up to) 4000 Å, in the significant majority of optimized systems they are less than 2000 Å. Clearly there is an orthovariance penalty to be paid by much wider filters.

Figure 8 goes further to explain why broad filters may be desirable. It shows that the effects on the SED of varying any of the four APs are coherent over a wide wavelength range and not restricted to specific, narrow wavelength intervals. Thus on signal-to-noise grounds – and subject to the orthovariance requirement – broader filters are more sensitive to AP variations[4]. This can be exploited by Gaia because, unlike ground-based surveys which are often limited by imperfect calibration of variable telluric effects, Gaia can make reliable use of the stellar continuum and unresolved features.

Another property often seen is overlapping filters. Large amounts of overlap are not desirable from the point of view of colour–colour diagrams. However, colour–colour diagrams are probably not the optimal way of determining stellar parameters. After all, such diagrams only make use of two or three bands (the normalization already being provided by the G band), whereas HFD is performing a separation directly in the higher dimensional space (five dimensions in this case, ten for MBP). This is likely to make a more efficient use of multivariate data than do colour-colour diagrams, which, from the point of view of stellar parametrization, are only a means to an end.

To get a better idea of how HFD works, we may investigate the evolution of the filter system parameters. There is immediately a difficulty here because for $I = 5$ filters there are formally $3I - 1 = 14$ independent parameters, the joint evolution of which cannot be visualized. Instead, Fig. 9 shows the evolution of each parameter type separately for a typical run. The central wavelengths occupy the full range of possible values throughout the evolution, although after 40–70 generations they show more concentration around a handful of values. Changes can be correlated with changes in the fitness evolution (Fig. 4). In contrast to this behaviour, within 10 generations most filters with a *HWHM* more than about 2000 Å are purged from the population only to make short-lived reappearances. This self-regulation property of HFD to remove very broad filters is frequently observed.

The fractional integration time, t, shows a much more continuous distribution between its bounds. This may indicate that the exact setting of t is not that critical. To test this I repeated the set of 20 runs with t fixed at 0.2 for all filters. The median fitness of the run maxima is about 4% lower and the filter systems are similar in their general properties. If, instead, the fractional integration times of the fully optimized system (Fig. 6) are set to 0.2 and the fitness recalculated, the fitness is found to be about 12% lower. With BBP on Gaia, six CCD slots may be available, enabling us to allocate two slots (i.e. $t = 2/6$) to the filter with largest t and 1/6 to the rest. With this discretization, the fitness decreases by less than 2% relative to the full optimization. In conclusion, optimizing t is desirable, but moderate rounding to match discrete CCD widths may not significantly degrade performance.

We can obtain a better idea of the performance of a filter system by looking at the distributions of the four AP-gradients and six orthovariance terms comprising the fitness, as shown in Figs. 10 and 11. In the AP-gradient calculation the full range of each AP is normalized to the range 0–1. Therefore, if we want a 2.5% difference in APs (e.g. 0.1 dex in [Fe/H] or $\log g$, or 0.25 dex in A_V) to be separated by a *SNR*-distance of at least 5, then we require AP-gradients of at least $5/0.025 = 200$. We see that this is easily achieved (at this G magnitude) for $T_{\rm eff}$

[4] This would not be true for APs which have a very localized wavelength signature, such as specific element abundances.

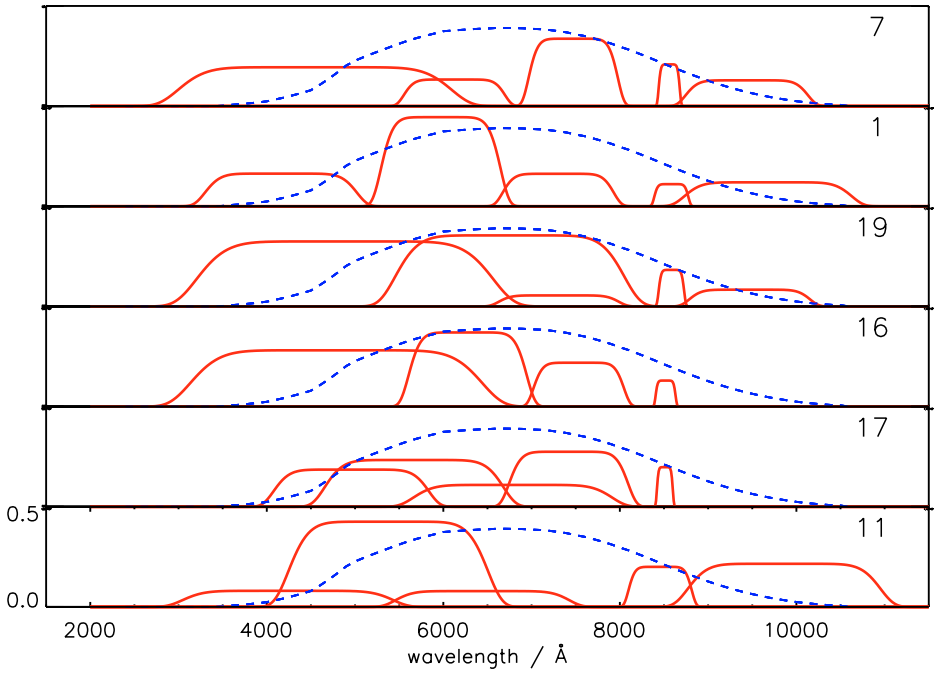

Fig. 7. The optimized BBP filter systems for six different runs (six different initializations), selected to show maximum variance between the filter systems (plotted as in Fig. 6). They are ordered from fittest (at the top, same as Fig. 6) to the least fit (at bottom). The run numbers in each panel correspond to those in Fig. 5.

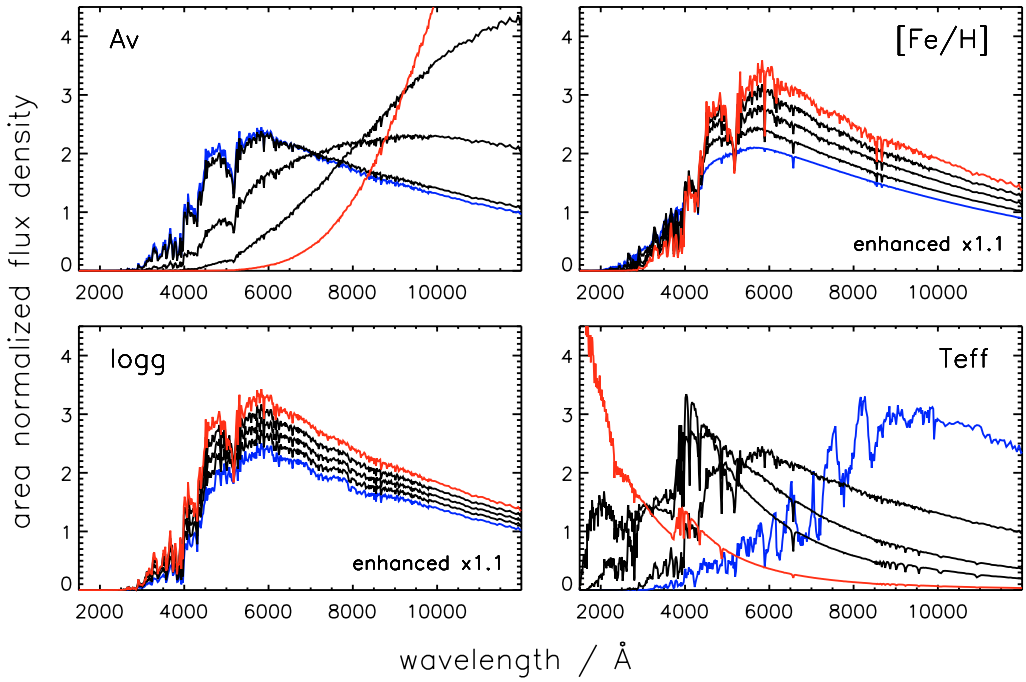

Fig. 8. Variations of the four APs have broad band effects. Taking the SED with APs $A_V = 0.0$ mag, [Fe/H] = 0.0 dex, $\log g = 4.5$ dex, $T_{\rm eff} = 4750$ K, each panel shows the effect of varying one AP over the full range shown in the grid (Table 2). The magnitude of the effects of $\log g$ and [Fe/H] have been enhanced for clarity by multiplying the five SEDs by 1.0, 1.1,..., 1.4. The SEDs are plotted to have equal integrated flux density over the wavelength interval 900–12 000 Å.

and A_V for essentially all sources but is not for $\log g$ or, especially, [Fe/H], for many sources. At some level this is to be expected, since $\log g$ and [Fe/H] are "weak" APs compared to $T_{\rm eff}$ and A_V. Yet differential weighting of these APs was used in the fitness function (Table 1) to make the optimization more sensitive to these APs. Clearly, these weak parameters still present a problem for a 5-filter BBP system at $G = 15$.

Mean AP-gradients up to 10–35% higher (depending on the AP) are found with the best filter systems from other runs. In other words, filter systems which have a lower fitness may

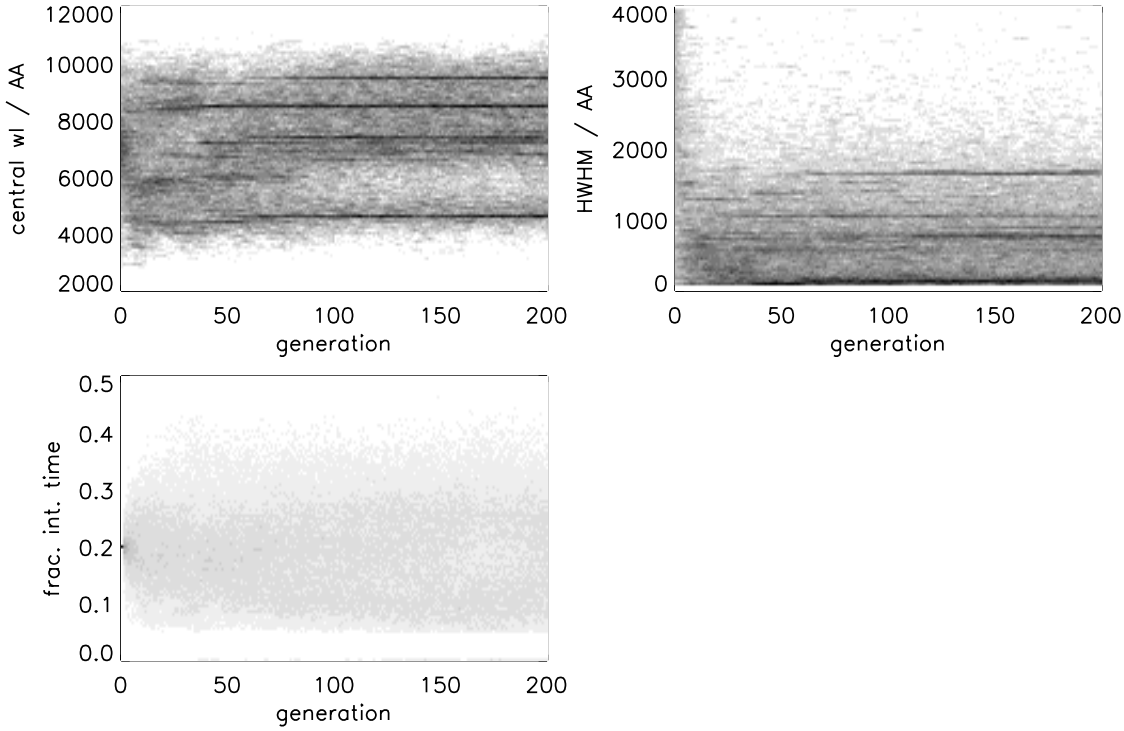

Fig. 9. Evolution of all filter system parameters for the nominal BBP setup with $I = 5$ filters for a typical run (the corresponding fitness evolution is shown in Fig. 4). At each generation the $I \times K = 1000$ values for that filter parameter type are plotted as a grey scale (with square root intensity scaling used to enhance sparse regions).

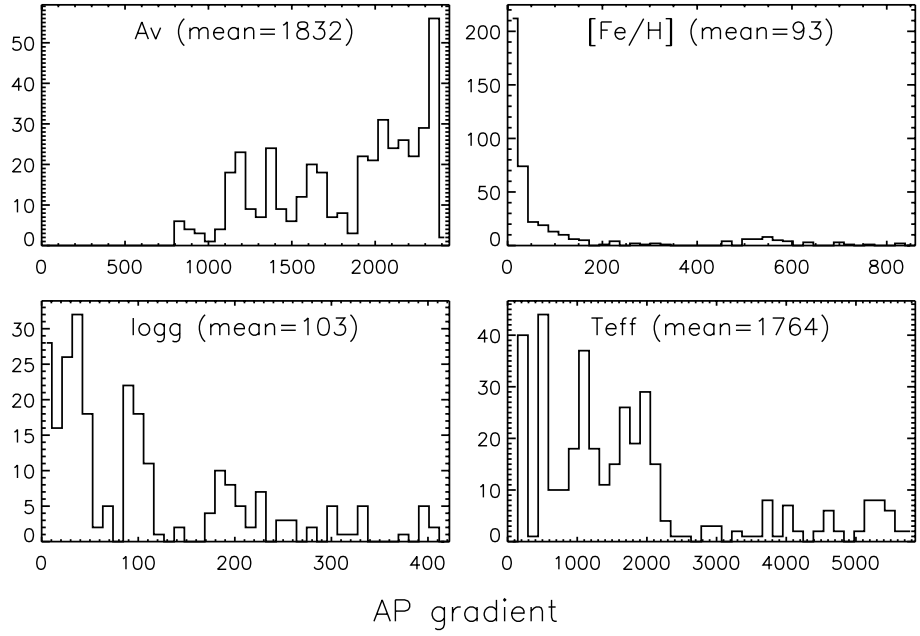

Fig. 10. Distributions of the four AP-gradients for all sources in the grid produced by the BBP filter system shown in Fig. 6. The mean values of the distributions are given. For comparison, these values averaged over 1000 random filter systems are: $A_V = 1435$; [Fe/H] = 49; $\log g = 68$; $T_{\rm eff} = 1461$.

nonetheless perform much better on a subset of the problem (e.g. for some APs or a subset of sources). This is almost inevitable when optimizing a fitness function which is an aggregate of many separate objectives. I shall return to this point in Sect. 5.

Figure 11 shows the distribution over the six orthovariance terms. Recall the transfer function used to give higher weight to $\sin\alpha > 0.95$ (Eq. (9)). HFD shows some success in achieving this high degree of vector separation in five of the six terms. However, in these cases many sources are still poorly separated,

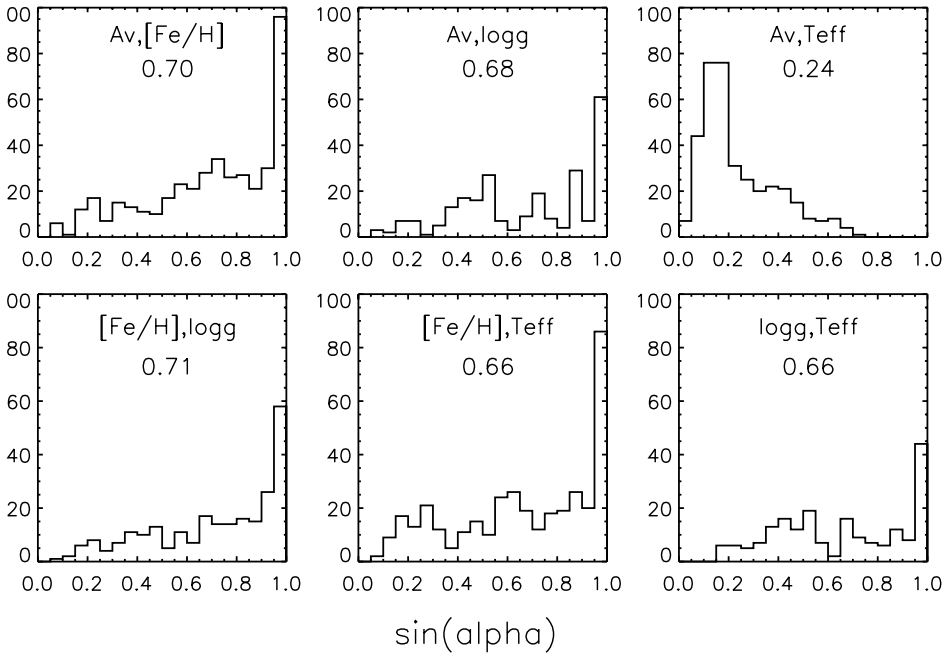

Fig. 11. Distributions of the six orthovariance terms ($\sin\alpha$) for all sources in the grid produced by the BBP filter system shown in Fig. 6. The mean values of the distributions are given. For comparison, these values averaged over 1000 random filter systems are: A_V, [Fe/H] = 0.52; A_V, $\log g = 0.47$; A_V, $T_{\rm eff} = 0.18$; [Fe/H], $\log g = 0.51$; [Fe/H], $T_{\rm eff} = 0.50$; $\log g$, $T_{\rm eff} = 0.46$.

and as the mean values correspond to $\alpha = 41°-45°$, significant degeneracy clearly remains. Furthermore, $T_{\rm eff}$ and A_V remain strongly degenerate for almost all sources, with a mean angle of only 14°[5].

To put this performance in context, and to assess the efficiency of the HFD search and selection procedure, we look at the performance of random filter systems. These achieve reasonable AP-gradient separation for $T_{\rm eff}$ and A_V (caption to Fig. 10). This is perhaps not that surprising given the broad band effects of APs (Fig. 8), because the filter systems are randomized between the limits listed in Table 1 so will include many wide filters. But the random systems perform somewhat worse on [Fe/H] and $\log g$: the optimized systems increase these AP-gradients by 90% and 50% respectively. Likewise the six orthovariance terms in the optimized system larger by factors of about 1.4 with respect to random systems.

4.3.2. Model parameter variations

Number of filters. The baseline Gaia design calls for 4–6 filters in BBP on the grounds of the chromatic correction for the astrometry (Sect. 4.2). A system of five filters was optimized above. While HFD can reduce the number of effective filters (by assigning zero integration time), it cannot add filters. The 20 runs were therefore repeated using 10 filters (and with the lower and upper limits on t set to 0.025 and 0.4 respectively). Of the resulting run maxima systems, 18 had 8−10 effective filters, although in several cases just a few filters receive most integration time or there were some near-identical filters. The other two filter systems had seven filters. These were not only the fittest two systems, but they also closely resemble the fittest filter systems from the 5-filter optimization plus two additional filters with low t. The fitnesses of these 20 run maxima lie in the range 22.3−24.8, i.e. slightly lower than the 5-filter optimization. Inspection of the distributions of the fitness terms (cf. Figs. 10 and 11) for the two 7-filter systems shows that while they have lower mean AP-gradients than the 5-filter systems, they have very slightly higher orthovariance factors. This is even the case for some of the less fit systems with more filters. Thus extra filters could contribute to improved vector separation at the price of lower AP-gradients.

Magnitude. The end of Sect. 3.2 discussed the dependence of the fitness on the source magnitude. Repeating the 5-filter optimization at $G = 20$ gives very different results: the seven fittest systems consist of only two effective filters and the remaining 13 systems of three. The AP-gradients are much lower than expected from just scaling from the $G = 15$ results based on Poisson noise, indicating that $G = 20$ is already the faint star limit for some filters. The systems with fewer than four filters of course cannot determine four APs independently. We may conjecture that these filter systems are sensitive to fewer than four of the APs. However, this is not born out by inspection of the distributions of the orthovariance factors, which are all decreased by similar amounts (>0.1). Clearly, HFD is unable to find useful solutions when optimized on data at $G = 20$. However, if the fitness terms for systems optimized at $G = 15$ are recalculated at $G = 20$, then we find that the orthovariance terms are only reduced by a few percent (see Sect. 4.5). Perhaps in the faint star limit the fitness space is dominated by strongly attracting, poor optima.

[5] Interestingly, if a filter system is optimized only on A_V and $T_{\rm eff}$ (but with the grid unchanged), then the mean value of this $\sin\alpha$ is increased to 0.34. This is also the only time that any sources (ca. 40) are seen with $\sin\alpha > 0.95$. Thus HFD does show some ability to find filter systems which partially break the A_V, $T_{\rm eff}$ degeneracy.

Grid. The HFD filter systems are of course very dependent on the stellar grid. By way of illustration, if we restrict the grid to stars with $T_{\rm eff} < 8000$ K, the optimized filter systems allocate more integration time to the bluest filter, presumably to compensate for the reduced flux in this wavelength range for the average star. The AP-gradients for $A_{\rm V}$, $\log g$ and [Fe/H] are now 20–80% higher than those obtained with the full grid. (The AP-gradients for $T_{\rm eff}$ are of course lower, because a given *SNR*-distance translates to a smaller AP-gradient on account of the normalization of ϕ in Eq. (3).)

Filter profile. Repeating the optimization with rectangular filter profiles increases the typical run maximum fitness by about 5%. This is attributed mostly to larger AP-gradients rather than to the orthovariance terms, which show negligible difference. The parameters of the optimized filter systems are very similar to those obtained with the nominal profile. The use of profiles with steeper sides therefore does not help the vector separation (at the level of separation achieved here).

Elitism. If elitism is not used ($E = 0$), the evolution is very different because the fittest systems are not forcibly retained. The maximum fitness now evolves in a similar erratic fashion to the minimum fitness seen in Fig. 4. Correspondingly, the evolution of the filter system parameters shows no convergence (no "lines" as in Fig. 9), indicating a lack of selection pressure. The run maximum is often found (and lost) within the first few tens of generations. These generally have a fitness around 15% lower than the run maxima attained when using elitism: it is clearly desirable to force the retention of the best solutions to await favourable offspring. In contrast, if $E = 100$ (half the population), the run maxima fitnesses are more tightly bunched (24.9–26.1 compared to 23.4–26.1) and there is a much higher degree of consistency across the corresponding filter systems, although the maximum fitness across 20 runs is no higher. Increasing the size of the elite is therefore desirable, as it increases the reliability of the outcome and so reduces the need to perform as many separate runs. Of course, increasing E beyond some point will be counterproductive as it leaves fewer individuals available for search.

Population size. A sufficiently large population is required to maintain diversity. If the population is too small it quickly becomes dominated by a suboptimal filter system before there has been adequate opportunity for search. Increasing the size of the population (and the elite) by a factor of ten typically improves the run maximum fitness by only 4%.

Recombination. If mutation is used as the only search operator, the resulting filter systems are qualitatively unchanged, and the fitnesses (and mean values of the individual fitness terms) are no lower. This recombination operator is therefore redundant. This is not that surprising: randomly swapping a single filter between filter systems is not obviously useful when we consider that it is the combined effect of all filters which determines how well stars are separated. This is in contrast to some other EA representations which use crossover operators (see Appendix B) in which a parameter (gene) and its local neighbours have a joint expression somewhat independently of the other genes.

Mutation. HFD without mutation would not be useful, as only mutation creates new filters. But the HFD results are not very sensitive to the probability of mutation. If it is reduced by a factor of ten to 0.04 then the run maximum fitness is changed by less than 1%. Lowering the standard deviations of the mutations for all three parameter types by a factor of two likewise has a negligible effect on the final filter systems.

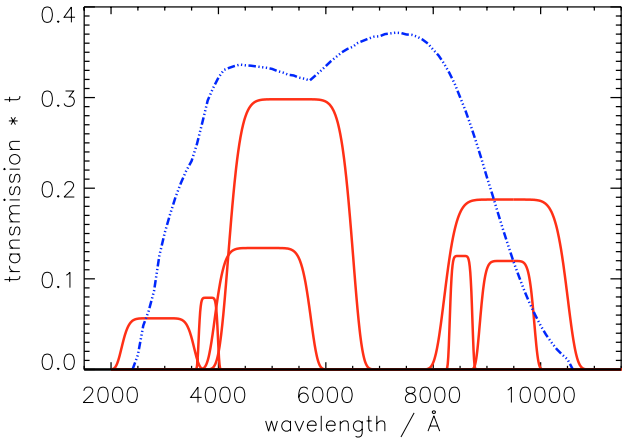

Fig. 12. The HFD-1M filter system, a MBP filter system produced by HFD (solid lines). The CCD+instrument response is shown by the dot-dashed line. See caption to Fig. 6.

4.4. Results: MBP

The main differences between the MBP and BBP instruments are shown in Table 1. MBP has a much larger integration time than BBP and is intended for detailed astrophysical characterization. A systems of 10 filters is initially considered.

The fitness evolution for MBP is qualitatively the same as for BBP, but now the run maximum fitnesses lie in the range 82–89, a factor of more than three above BBP. The AP-gradients are considerably larger than those found with BBP at the same magnitude, as expected due to the larger sensitivity for MBP at this magnitude. The orthovariance factors are similar to or larger than those found for BBP. The fittest filter system from a set of 20 runs is shown in Fig. 12. It shows a mix of broad and narrow band filters extending to the most extreme wavelengths permitted by the instrument/CCD response. There are some similarities to the BBP systems shown in Fig. 7, e.g. the relatively narrow filter around 8500 Å (see Table 3).

One may postulate that higher orthovariance factors could be achieved with narrower filters, as these could plausibly better discriminate between spectral features. This was tested by repeating the optimization with the maximum *HWHM* set to 400 Å. The result is that the orthovariance factors are increased by about 0.05 (more for $A_{\rm V}$, $T_{\rm eff}$), although not many more are put into the desired 0.95–1.00 range required to reasonably break the degeneracy. This also comes at the cost of reduced AP-gradients – as fewer photons are collected – although these are still adequate. Interestingly, the optimization does not force all the filter widths to the maximum permitted. The fitness is about 20% lower. The improvement in vector separation from narrow filters is therefore small (and the degradation in AP-gradients may not be acceptable at faint magnitudes). This is not surprising when we again consider that the effects

of AP variations are coherent over a wide wavelength range (Fig. 8).

Many of the HFD-optimized MBP systems include filters with only a small allocation of fractional integration time, t. It is therefore tempting to think that such filters could be removed and their integration time allocated to other filters, but in fact this frequently results in a dramatic decrease in the fitness. (This is the case for the HFD-1M system, for example.)

The optimization leading to HFD-1M was done with 10 filters, but there are only 7 effective filters in this optimized system. Across the set of 20 runs, two had 7 effective filters, one had 8 and the rest 9 or 10, although those with 9 or 10 filters often have two or more very similar or extensively overlapped filters. If the optimization is repeated with 15 nominal filters, the run maxima fitnesses and orthovariance terms are similar or slightly lower than with 10 nominal filters. With only 5 nominal filters in the MBP optimization, the resulting systems sometimes have slightly higher fitness than the nominal 10-filter MBP systems. However, they have smaller orthovariance factors, which, given that the 10-filter systems already achieve adequate AP-gradients, is more significant.

In conclusion: at the level of separation currently achieved, 7 or 8 filters in MBP are an optimal trade off between spectral sampling and sensitivity for the grid in Table 2.

4.5. Comparison with other photometric systems proposed for Gaia

The HFD fitness function is a general figure-of-merit and can be calculated for any photometric system. A number of other photometric systems have been designed for Gaia. The present main candidates are the BBP 2B system (Lindegren 2003) consisting of 5 broad, partially overlapping filters and, for MBP, 2F (Jordi et al. 2003) and 1X (Vansevicius & Bridzius 2003), both consisting of relatively narrow filters to measure specific stellar features (Fig. 13). The fitness terms have been calculated for these filter systems using exactly the same instrument models and grid as used for the HFD optimization. Table 4 lists the fitness terms and compares them with the HFD systems.

For BBP, HFD-1B has almost twice the fitness as 2B although only two of its AP-gradients are higher. Its higher fitness is due to the fact that it has quite a few more sources with orthovariance terms in the desired range 0.95−1.00, which is given more weight in the fitness due to the transfer function (Eq. (9)). This difference between the distributions is not represented by the only slightly higher (unweighted) mean values in Table 4 for the orthovariance terms for HFD-1B.

Turning to MBP, HFD-1M is 2.6 times fitter than either 1X or 2F. HFD-1M achieves much higher AP-gradients by virtue of its wider filters. It has slightly lower mean orthovariance terms than does 1X. This agrees with what was observed with HFD systems (Sect. 4.4), namely that narrower filters can achieve better vector separation, although in both cases the improvement is small. More importantly, 1X has only slightly more sources with orthovariance terms in the range 0.95−1.00 than does HFD-1M (and the latter actually has more values of $\sin\alpha(\log g, T_{\rm eff})$ in this range). As this is the range

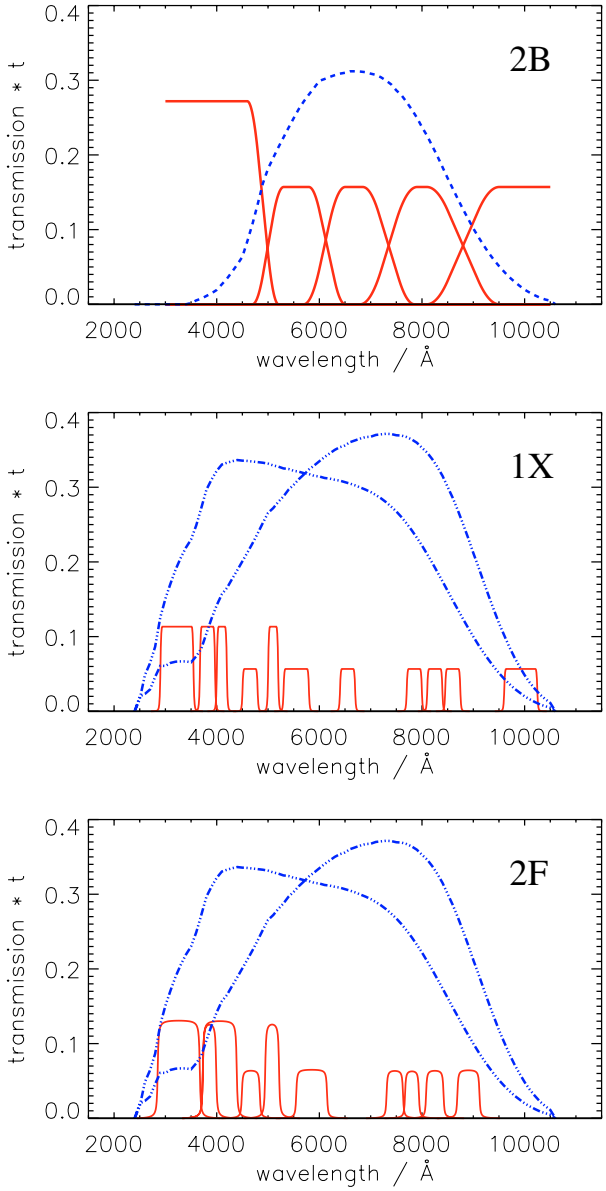

Fig. 13. Three filter systems proposed for Gaia by previous authors. The filter profiles have been plotted in the same way as in Fig. 6 to show the fractional integration times. Over plotted in each case are the CCD sensitivities. 2B is a BBP system; 1X and 2F are MBP systems.

we are primarily interested in (as only then can we say that degeneracy has been satisfactorily minimized), we see that 1X is little better than HFD-1M at vector separation. Only for $A_{\rm V}$, $T_{\rm eff}$ does 1X achieve a much higher mean, although it too has no sources in the 0.95−1.00 range. Thus 1X – like HFD-1M – has failed to break the degeneracy between extinction and effective temperature. Comparing HFD-1M with 2F, the latter has slightly fewer sources in the 0.95−1.00 range than the former so is slightly worse at vector separation.

If the fitness terms are recalculated at $G = 20$, then the fitnesses of all filter systems are reduced by a similar factor. The AP-gradients of course decrease a lot as they are just proportional to the *SNR*. For HFD-1B the mean values are 60, 3, 3, 57 (order as in Table 4); for HFD-1M they are 281, 10, 13

Table 4. Fitness comparison of the two HFD filter systems HFD-1B and HFD-1M and three other systems proposed for Gaia (Fig. 13). The overall fitness as well as the mean values (averaged over the sources in the grid) of the AP-gradients and the orthovariance terms are shown. The quantities are calculated with all sources at $G = 15$.

	HFD-1B	2B	HFD-1M	1X	2F
Fitness	26.1	13.7	89.4	34.6	34.2
$h(A_V)$	1832	1944	7206	3183	3932
h([Fe/H])	94	72	272	195	226
$h(\log g)$	103	86	337	240	261
h($T_{\rm eff}$)	1765	1888	6827	3177	4095
$\sin\alpha(A_V$, [Fe/H])	0.70	0.66	0.70	0.76	0.73
$\sin\alpha(A_V, \log g)$	0.68	0.60	0.75	0.81	0.77
$\sin\alpha(A_V, T_{\rm eff})$	0.24	0.24	0.21	0.40	0.40
$\sin\alpha$([Fe/H], $\log g$)	0.71	0.61	0.73	0.73	0.71
$\sin\alpha$([Fe/H], $T_{\rm eff}$)	0.66	0.63	0.68	0.70	0.66
$\sin\alpha(\log g, T_{\rm eff})$	0.66	0.60	0.75	0.77	0.73

and 263. The values are correspondingly lower for the other filter systems. For BBP these all fall well below the desired value of around 200 (see Sect. 4.3.1), so good scalar separation is not possible for many stars with BBP at the limiting magnitude of the survey. For MBP, good scalar separation is possible at $G = 20$ for extinction and effective temperature, but not for metallicity or surface gravity. (This should only be taken as a rough indication, however, because in parts of the grid AP-gradients much less than 200 are acceptable, e.g. for [Fe/H] in hot stars.) At $G = 20$ the orthovariance factors are only decreased by a few percent with respect to $G = 15$. This is what we would expect as the principal directions are little affected by the *SNR*.

In summary, we find that the two HFD systems perform as well as or better than their "classical" (2F, 2B, 1X) counterparts. Nonetheless, there are still some poor aspects of the HFD (and classical) filter systems, the possible cause of which will be discussed in the following section. Once these have been improved upon, a more detailed assessment of the parametrization performance of the HFD systems using standard methods (e.g. Bailer-Jones 2000) will be warranted.

5. Discussion: HFD assumptions and improvements

A critical analysis of HFD follows to highlight the underlying assumptions and weaknesses of the approach, along with suggestions of how it may be improved.

HFD as implemented in this article is concerned only with determining stellar parameters. In a survey, the same filter system must also distinguish single stars from the "contaminants", such as quasars, unresolved galaxies and unresolved binary stars. (With Gaia, some assistance in this task comes from the astrometry.) The filter system could be simultaneously optimized to distinguish such contaminants by adding an extra term to the fitness which is the sum of *SNR*-distances between each contaminant and each source in the grid. Maximizing this places the contaminants away from the sources of interest.

The filter systems produced by HFD depend on the grid of APs, the SEDs used to represent the stars and the weights set for each AP. As the fitness is just a sum over all sources, the relative distribution of different types of stars is significant and must be carefully considered. Note also that the fitness sum (Eq. (8)) may be generalized to include different weights for each star or even for each AP of each star.

It should be emphasized that the present fitness function is concerned only with a *local linear* separation of sources in the multidimensional filter space. If successful, it means that only locally linear regression models are necessary to calibrate this data space in terms of APs, allowing considerable simplifications. Higher order terms could be included in the fitness function and generally one would expect this to give rise to superior filter systems – or at least a more accurate determination of the fitness – at the cost of a more complex optimization. Calibration would correspondingly require locally nonlinear regression methods. A further complication which is ignored in HFD is the possible presence of *global* degeneracies of APs, i.e. disjoint parts of the AP space overlapping in the data space. Ideally the fitness function should be further modified to measure the extent of this and penalize against it.

The grid used (Table 2) is relatively sparse in the APs. This is probably adequate from the point of view of sampling the dependence of the data on the APs. However, this same grid is used to provide the neighbours (the isovars; see Fig. 2) for determining the fitness at each grid point. HFD therefore implicitly assumes that the photon counts vary linearly with the APs on the local scale between a source and its isovars. This assumption may not be valid for all points in the grid. It could be avoided by using a second, denser grid from which the isovars are selected to better satisfy the local linearity assumption[6].

One of the major limitations of the HFD filter systems (and the others considered in Sect. 4.5) is that they give relatively poor vector separation for many stars, i.e. APs remain degenerate in parts of the grid. It remains to be analysed in detail whether these are regions of the grid which are intrinsically degenerate for medium and broad band photometry, or whether HFD is simply unable to create suitable filters systems. As the fitness function is an amalgamation of different terms (4 AP-gradients and 6 orthovariances), there is a danger that a high fitness be achieved by increasing some terms with little regard to others, i.e. the optimization becomes desensitized to some of the fitness terms. This will be returned to below. This is likewise a problem for different sources: a high fitness could be achieved by overseparating some sources while underseparating others.

An alternative explanation for poor vector separation is that the search operators are not searching the parameter space efficiently. An efficient, directed (rather than random) search is important because there is a very large number of potential filter systems, as a simple calculation makes clear. Suppose that only differences in central wavelength by at least 100 Å are

[6] Needless to say, nothing is gained if this second grid is constructed by linearly interpolating the first grid.

significant. In this case, the wavelength range 4000–10 000 Å contains only 60 different central wavelengths. Applying the same step size to *HWHM* increments of up to 1500 Å gives 15 discrete filter widths. Even if we ignore variation in the fractional integration times, for a system of 5 filters there are of order 10^{14} different combinations of filter parameters and of order 10^{29} for systems with 10 filters, of which only a negligible fraction can be ignored as being obviously inappropriate. In contrast, HFD evaluates around 10^5 filter systems during an optimization run.

Provided the offspring of fitter parents are generally fitter than the offspring of less fit parents (which has been experimentally confirmed with HFD), the population will evolve toward fitter solutions (Hinterding 2000). Elitism then guarantees that the optimum is found (eventually). If the fitness convergence seen in Fig. 4 is asymptotic, then the search operators are working well, i.e. the solutions we find are about the fittest available. However, it could be that some specific changes of the filter system parameters produce a significant increase in fitness. If this is the case, then more directed search operators may be useful. One possibility is to use a hybrid stochastic/gradient search method. Another is to use *strategy parameters* to adapt the size of the mutations as the evolution proceeds (see Appendix B). I attempted a variation of this which reduced the mutation sizes for a single filter system if its fitness decreased – the rationale being that as an optimum is approached a more refined search should be undertaken – but this did not lead to improvement.

These considerations aside, my feeling is that the most significant limitation of HFD is the fact that it consists of only a single objective function. It cannot be overemphasized that our goal is really to simultaneously maximize ten separate fitness terms: 4 AP-gradient and 6 orthovariance terms (each averaged over the sources in the grid). Equations (6) and (10) is but one way to amalgamate these into a single objective function, albeit with some justification. Nonetheless, it can result in less fit filter systems yielding higher values for some fitness terms than do fitter filter systems, as was seen earlier. For example, the optimum from run 19 in Fig. 7 achieves AP-gradients 5–20% higher than the fittest filter system (run 7 in the same figure), yet its fitness is 4% smaller due to lower orthovariance factors. How can we properly compare two filter systems which have very similar overall fitnesses, yet one performs better at some aspects and worse at others? In principle, the fitness function is suitably constructed and weighted to increase monotonically with increasingly "better" filter systems. But can we uniquely establish in advance what "better" means? Not only is it very difficult to determine an appropriate weighting a priori, it is strictly not possible. This is because (a) we cannot compare different types of measures (e.g. AP-gradients and orthovariance terms) on an equal footing, (b) the scientific criteria may not give rise to a unique weighting, yet the optimum solution may be quite sensitive to this weighting, and (c) any attempt to weight terms a priori requires that we have some idea of what degree of separation is even possible within the constraints of the instrument and grid, yet this is something we generally do not know in advance. Thus a single fitness function could easily set conflicting or unattainable requirements on the different terms.

A solution to this dilemma is available through the use of multiobjective optimization methods (e.g. Deb 2001). This approach avoids comparing dissimilar objective functions by optimizing each separately. The goal is not to arrive at a single solution, but at a set of so-called "non-dominated solutions". A non-dominated solution is one for which no other solution exists which has higher values of all objective functions. The non-dominated set of solutions over the entire search space is called the "Pareto optimal set", solutions which are better than all other possible solutions in all objectives, but are only better than each other in some respects. They are, therefore, the best possible set of compromise solutions. Having found these we can reassess the scientific requirements in terms of what is actually possible within the optimization constraints and select the most desirable compromise.

6. Summary and conclusions

I have introduced a novel approach to the design of photometric systems via optimization of a figure-of-merit of filter system performance. In the present incarnation, this figure-of-merit (or fitness) measures the ability of a filter system to determine multiple stellar astrophysical parameters (APs), by calculating the separation in the data (filter) space between stars with different APs. The better that sources can be separated (in signal-to-noise units) according to their AP differences, the better the filter system. This separation is vectorial in nature, meaning that the figure-of-merit is also proportional to the angle between the vectors which define the directions of local variance of each AP: in the ideal filter system these vectors would be mutually orthogonal at all points in the AP space, thereby removing any degeneracy between APs. The fitness is calculated via an instrument model for a grid of spectra, which sample stellar parameters the photometric system must determine.

The optimization is performed with an evolutionary algorithm. In this approach, a population of filter systems is evolved according to the principle of natural selection, such that the fitter filter systems are more likely to survive and to produce more "offspring". Reproduction takes place by combining or mutating selected parents, resulting in changes of the filter parameters (central wavelength, profile width, integration time), thus providing a stochastic yet directed search of the filter parameter space.

This model, HFD (Heuristic Filter Design), has been applied to design CCD photometric systems for the Gaia Galactic Survey Mission. The systems were optimized to separate the four APs effective temperature, $T_{\rm eff}$, metallicity, [Fe/H], surface gravity, $\log g$, and interstellar extinction toward the star, $A_{\rm V}$. Recurrent characteristics of the resulting filter systems are broad overlapping filters, although filters with a half-width above 1500 Å were consistently disfavoured. The preferred broadness is not surprising when one realises that each of the APs has a coherent effect on the data over a wide wavelength range. Narrower filters were found not to improve significantly the orthogonality (vector separation). This tendency toward broader filters than have hitherto been adopted for the Gaia filter systems – and for stellar parametrization in general – is one of the main results of this application of HFD. Likewise

is the related tendency toward overlapping filters. This may be indicative of a more efficient use of a multi-dimensional data space than non-overlapping systems.

In terms of the scalar separation of sources, the HFD filter systems perform well at the Gaia target magnitude of $G = 15$, although at the limiting magnitude of $G = 20$ the separation for [Fe/H] and $\log g$ is unsatisfactory. More significantly, the vector separation is inadequate in parts of the AP grid, and between $T_{\rm eff}$ and $A_{\rm V}$ in particular considerable degeneracy remains. Yet other systems proposed for Gaia show similar difficulties, and overall HFD performs at least as well as or better than these. It remains to be seen whether these are intrinsic limitations of broad and medium band photometry for these instrument models or whether improvements to the fitness function alter this. Either way, this systematic approach to filter system design embodied in HFD shows considerable promise.

A number of improvements to HFD to address some deficiencies were suggested, including the use of more efficient search operators, the use of secondary grids or generalization to nonlinear separation, and the incorporation of multiobjective optimization methods. The latter allows the different objectives of the filter system to be optimized separately, thus avoiding having the problem of weighting and combining heterogeneous objectives.

Specifically with regard to Gaia, HFD may be developed in a number of ways. The most significant is perhaps the inclusion of parallax information: the parallaxes from Gaia will permit an accurate determination of the luminosity and (via $T_{\rm eff}$) the radius of many stars, reducing the need to determine $\log g$. By including the parallax error model in HFD, filter systems better matched to the available astrometry can be designed.

Beyond this application, HFD represents a generic approach to formalizing filter design by casting it as an optimization problem with few prior assumptions. The key steps are the parametrization of the filter system, the construction of a figure-of-merit, and the design of appropriate genetic operators to search the parameter space. Evolutionary algorithms are particularly appropriate for this problem because the fitness landscape in which the optimization is performed is frequently complex and noisy. While these steps are nontrivial, HFD provides a general framework for applying this approach to many other problems. These include the identification of particular types of objects, such as ultra cool dwarfs or metal poor stars, star/quasar separation, the spectral classification of galaxies, and photometric redshift determination. This is applicable not only to future large scale surveys, but also for more modest surveys on existing ground-based facilities.

Acknowledgements. I would like to thank Anthony Brown, Jos de Bruijne, Lennart Lindegren and Michael Perryman for useful suggestions and discussions during the development of HFD. I particularly acknowledge input and constructive criticism from Jos de Bruijne in the early stages of this work. Thanks also to Carme Jordi for information concerning the instrument model. I am especially grateful to Bob Nichol and the Astrostats group at Carnegie Mellon University for access to significant amounts of computer time and for general support during my time in Pittsburgh.

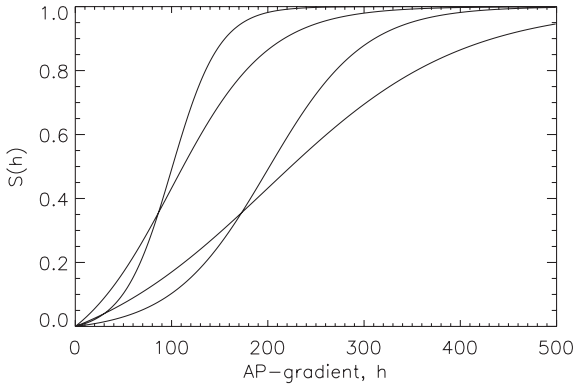

Fig. 14. A transfer function for the AP-gradients, given by Eq. (11). From left to right at the top of the plot, the lines are for $\kappa = 100$, $\omega = 2$, $\kappa = 100$, $\omega = 4$, and $\kappa = 200$, $\omega = 2$, $\kappa = 200$, $\omega = 4$.

Appendix A: Fitness functions

HFD uses single objective optimization, requiring the aggregation of the AP-gradients and the orthovariance terms into a single objective function. This was achieved via the cross product (Eq. (5)). However, it was found advantageous to modify the basic form. First, the AP-gradients were raised to a fractional power (1/2) to avoid overseparation (a subset of sources dominating the fitness). Second, the four APs were assigned different weights to account for the fact that each has a different magnitude effect on the data. These two problems could in principle we avoided by using a transfer function to map the full range of the AP-gradient (zero to essentially infinity) to a restricted common range for all APs, say 0−1. One possible form is a modified sigmoid function

$$S(h) = \mathrm{e}^{-\omega}\left(\frac{1+\mathrm{e}^{\omega}}{1+\mathrm{e}^{-\omega(\frac{h}{\kappa}-1)}} - 1\right) \qquad (11)$$

shown in Fig. 14. $S(h)$ replaces $w_j h$ in Eq. (10). κ is the transfer point of the function and ω controls the sharpness of the transfer. As discussed in Sect. 3.2, $\kappa = 200$ is a reasonable target value for AP-gradients. Values of h well below this are assigned low fitness, and all values well above κ are assigned a similar fitness, thus avoiding overseparation. (With the AP-gradients now mapped onto the same range as the orthovariance terms, we could even avoid the cross product approach by simply summing the terms.)

The major problem with a transfer function is that it disregards what values of the APs it is even possible to achieve with the instrument model and grid. That is, simply assiging κ to achieve target values of h for some AP may force $S(h)$ into the unresponsive regions near 0 or 1, making all sources equally fit or unfit, thus depriving the fitness function of discriminative power. With $\kappa = 200$, $S(h)$ would be near 0 for [Fe/H] and $\log g$ for almost all sources, whereas it would be near 1 for $A_{\rm V}$ and $T_{\rm eff}$ for almost all sources (see Fig. 10). Thus not only would the fitness be indiscriminative, it would also be insensitive to [Fe/H] and $\log g$. Experimental testing of this transfer function confirms this. We cannot assign target values according to ideals to arrive at a useful fitness measure.

In contrast, the static weighting used in Eq. (10) brings all of the APs to the same "level" in the fitness function,

forcing the fitness and hence the selection operator to be equally sensitive to all APs. However, these static weights cannot be determined a priori as they depend not only on the grid and instrument model, but also on the typical AP-gradients and hence the filter system itself, thus demanding an unsatisfactory quasi-iterative approach.

The underlying problem of all of these approaches arises from the need to combine different objectives (AP-gradients, orthovariance terms) into a single fitness function which both takes account of the different effects they have on the data and ensures that they are equally represented. This is rather intractable, as the effects of the APs on the data depend on the filter system itself, just the thing we are trying to modify using the fitness. The way around this is not to combine the different objective functions at all, but to optimize each separately using multiobjective optimization methods (see Sect. 5). This would obviate several unsatisfactory aspects of the HFD model and the need for the above transfer function.

Appendix B: Evolutionary algorithms

There are many variants on how the genetic operators (selection, recombination and mutation) are implemented and, equally importantly, how the problem parameters (genes) are represented. Historically, the approaches can be split into at least three broad (and overlapping) categories: *genetic algorithms*, *evolution strategies* and *evolutionary programming*.

Genetic algorithms (GAs) typically use a binary representation for the genes, that is, each individual is represented by a string of binary digits. Recombination usually involves probabilistically selecting two individuals from the parent population, randomly choosing a point between two genes at which both individuals are split, and then recombining the left part of one with the right part of the other and vice versa, to create two new individuals. This is so-called "single point crossover". Repeating this for $\mu/2$ randomly selected pairs for a population size μ produces a new population. Mutation takes a comparatively background role, randomly flipping one or more genes with low probability to avoid stagnation.

Evolution strategies (ESs), on the other hand, usually use real-valued representations, i.e. K real-valued genes. Recombination may be used, but mutation is often a more significant operator: it is applied to all μ individuals in producing the intermediate population, usually by adding a Gaussian random variable $N(0, \sigma_k)$ to the kth gene. Another feature of the canonical ES is that these mutation parameters, $\{\sigma_k\}$ (the so-called *strategy parameters*), are themselves mutated at each generation, a procedure referred to as *self adaptation*. In other words, the typical mutation sizes are themselves subject to natural selection. This may even be extended to include covariance strategy parameters. Selection is usually deterministic with ESs, either using (μ, λ) selection, in which an offspring population of size λ is produced and the μ fittest individuals are selected, or $(\mu + \lambda)$ selection, in which the μ fittest individuals are selected from the union of the λ offspring and the μ parents. These are highly elitist strategies.

Evolutionary Programming (EP) is closely related to ESs, the two main differences being the employment of probabilistic selection and the exclusive use of mutation in EPs.

This broad distinction into ESs, GAs and EPs is largely historical and many applications now draw upon elements of each. HFD is no exception in this respect.

Since the introduction of what are now collectively called evolutionary algorithms for optimization in the 1950s and 1960s, they have undergone considerable development and have been applied in a variety of fields. There is a vast literature on GAs, ESs and EPs. An introduction to all three types of evolutionary algorithm can be found in Bäck & Schwefel (1993) or Fogel (1995), with more comprehensive information on many aspects provided by the collection of articles edited by Bäck et al. (2000a, 2000b). A good introduction to GAs in a broad sense is Mitchell (1996) and one of the classic, most cited works in this field is Goldberg (1989). A discussion of the analogies employed in GAs (and simulated annealing) can be found in Bailer-Jones & Bailer-Jones (2002).

References

Bäck, T., & Schwefel, H.-P. 1993, Evolut. Comp., 1, 1

Bäck, T., Fogel, D. B., & Michalewicz, T. 2000a, Evolutionary computation 1, Basic algorithms and operators (Bristol: IoP Publishing)

Bäck, T., Fogel, D. B., & Michalewicz, T. 2000b, Evolutionary computation 2, Advanced algorithms and operators (Bristol: IoP Publishing)

Bailer-Jones, C. A. L. 2000, A&A, 357, 197

Bailer-Jones, C. A. L. 2002, Ap&SS, 280, 21

Bailer-Jones, C. A. L. 2003, in ASP Conf. Ser., ed. U. Munari, 298, 199

Bailer-Jones, D. M., & Bailer-Jones, C. A. L. 2002, in Model-based reasoning, ed. L. Magnani, & N. J. Nersessian (New York: Kluwer/Plenum), 147

Deb, K. 2001, Multi-objective optimization using evolutionary algorithms (Wiley)

ESA 2000, Gaia: Composition, Formation and Evolution of the Galaxy, Technical report SCI(2000)4

Fitzpatrick, E. L. 1999, PASP, 111, 63

Fogel, D. B. 1995, Evolutionary computation. Toward a new philosophy of machine intelligence (New York: IEEE Press)

Goldberg, D. E. 1989, Genetic algorithms in search, optimization, and machine learning (Reading, MA: Addison-Wesley)

Hinterding, R. 2000, in Proceedings of the 2000 Congress on Evolutionary Computation, IEEE, Piscataway, N.J., 916

Jordi, C., Grenon, M., Figueras, F., Torra, J., & Carrasco, J. M. 2003, Gaia technical report UB-PWG-011

Lejeune, T., Cuisinier, F., & Buser, R. 1997, A&AS, 125, 229

Lindegren, L. 2001, Gaia technical report GAIA-LL-039

Lindegren, L. 2003, Gaia technical report GAIA-LL-045

Mitchell, M. 1996, An introduction to genetic algorithms (Cambridge M.A.: MIT Press)

Oke, J. B., & Gunn, J. E. 1983, ApJ, 266, 713

Perryman, M. A. C., de Boer, K. S., Gilmore, G., et al. 2001, A&A, 369, 339

Vansevicius, V., & Bridzius, A. 2003, in ASP Conf. Ser., ed. U. Munari, 298, 41